JOURNAL OF MATERIALS SCIENCE 32 (1997) 4693–4699

Growth of diamond films on SiC, WC and cubic BN substrates

J. ECHIGOYA, H. ENOKI*, S. KAMINISHI*
*Department of Materials Science and Technology, Faculty of Engineering, Iwate University Morioka 020, Japan and *Department of Materials Processing, Faculty of Engineering, Tohoku University, Sendai 980-77, Japan*

The growth morphology of diamond films grown on single crystals of SiC and on sintered WC and cubic BN (CBN) substrates by hot filament assisted chemical vapour deposition was examined using transmission electron microscopy and scanning electron microscopy. Diamond was found to have the form of particles on the substrates of SiC and WC in the initial stage of film growth. Both an amorphous layer and a directly bonded area were seen at the interface. Several orientation relationships, different from the cube/cube relation, were observed in these systems. On the other hand, in the case of diamond films on CBN substrates, the growth morphology of diamond was affected by the surface condition of the substrates. When CBN substrates were polished with a diamond paste before deposition, diamond grew in the form of particles. The growth morphology was changed by ion sputtering of the surface of the substrate from particle growth to uniform film growth. These results are discussed on the basis of lattice mismatch at the interface.

1. Introduction

The growth of thin diamond films at low pressure has been established by different methods that are relatively familiar [1]. Though it is well established that diamond films grow as the result of competition among the processes of nucleation, growth and the etching of diamond and non-diamond species, such as graphite and amorphous carbon [2, 3], the crystallography and microstructure of the resulting diamond films remain to be investigated. Recently, Ruhle *et al.* have shown the chemical effect on amorphous formation during the nucleation and growth of diamond films in a diamond/Si system [4]. Control of the nucleation and growth of diamond films on substrates is important for obtaining high quality films. Epitaxial growth of diamond films on different substrates is an attractive way to obtain high quality film and has been examined on diamond and CBN substrates, the latter having a lattice parameter very similar to that of diamond [5, 6]. However, a systematic study of the effect of substrates on the growth of diamond films does not seem to have been investigated yet. In this work, we report the growth of diamond films on SiC, WC and cubic BN substrates to investigate the effect of lattice mismatch of the substrate and the film. Single crystals were employed for the SiC and cubic BN substrates. Since cubic BN single crystals, used in the present experiment, were too small to use for electron microscopic observation, sintered CBN substrates were used to grow diamond films.

2. Experimental procedure

Diamond films were deposited on single crystal SiC substrates, sintered WC, and on single crystal and sintered CBN in a conventional hot filament assisted chemical vapour deposition system [3]. The conditions used in the present experiment were as follows: a substrate temperature of 900–1100 K; a filament temperature, W, of 2300 K; a ratio of methane to hydrogen of 0.5–1 vol %; a gas flow rate of 2×10^{-5} m^3 s^{-1}; and a pressure of 2.7 Pa. The cubic BN substrates were single crystals of particles with diameters of about 100 μm, which were fixed on a palladium plate before deposition. A single crystal of α-SiC, provided by Hoechst Japan Co., was cut and its (0 0 0 1) surface was polished prior to diamond film deposition. Sintered WC–Co alloys and cubic BN with about 50 vol % CBN, provided by Toshiba Tungaloy Co., were polished, and ion thinned from only the back side of the sintered materials. Transmission electron microscopy (TEM) was extensively employed for examining cross-sectional as well as plan-view samples. Conventional TEM specimens were prepared by ion thinning from the back side of the specimens. Cross-sectional specimens were prepared using the procedure outlined in a previous work [3]. Electron microscopy was performed employing a Jem 200B microscope and a Jeol 200CX high resolution microscope operating at a beam voltage of 200 kV.

3. Results

Fig. 1 presents a cross-sectional electron micrograph of a diamond film grown on scratched (0 0 0 1) SiC, using a diamond paste with a particle diameter of 1 μm, which shows that the diamonds grew as polycrystals. As seen in this micrograph of the interface, the SiC surface was irregular, not flat, and had steps of several atomic heights because of scratching by the

0022–2461

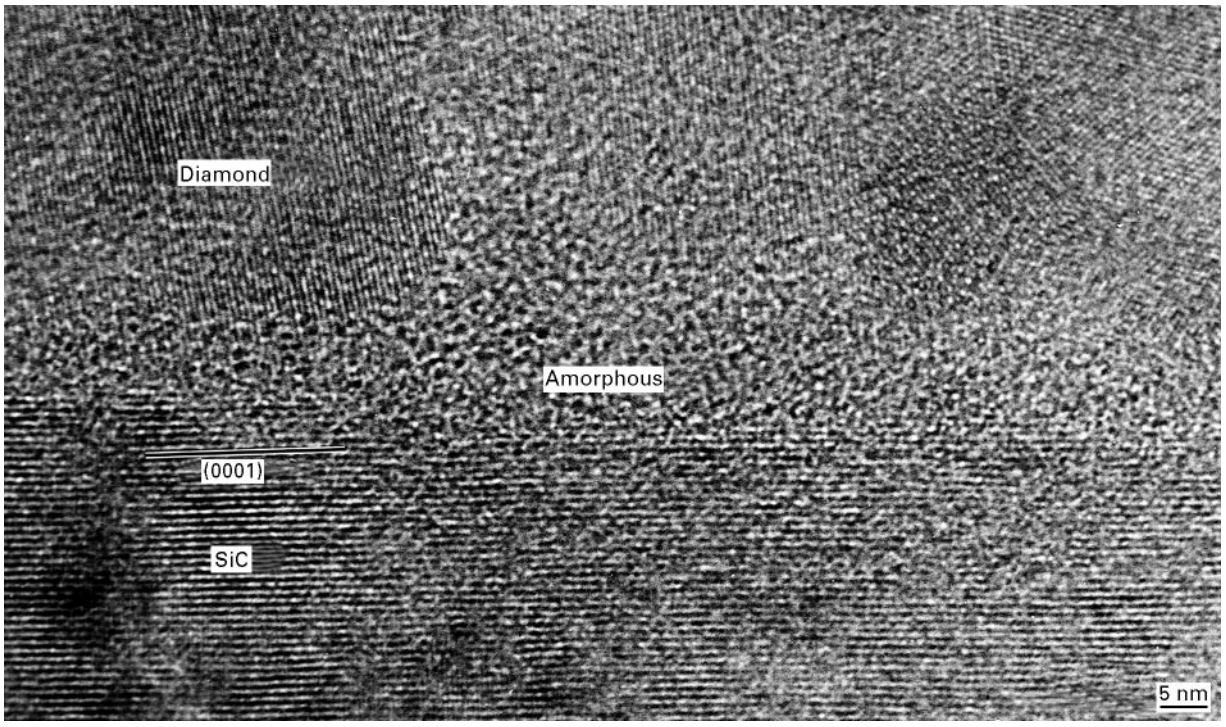

Figure 1 Cross-sectional electron micrograph of a diamond film grown on scratched (0 0 0 1) SiC using a diamond paste with a particle diameter of 1 μm.

diamond paste. Lattice fringes of the diamond film, which were mainly formed by the (1 1 1) lattice plane, revealed that the diamond film grew directly from the SiC substrate, though the area of contact was small and the film seemed to grow from the top of the SiC surface. This means that nucleation of the diamond film took place in a small area of the SiC, which was convenient for the nucleation of diamond. An amorphous phase seems to exist in the diamond film in the area between the grains near the interface. The diamond film includes twins. Though it is difficult to determine the orientation relationships and the exact interface structure from this image because of the observation of only one set of 1 1 1 lattice fringes of the diamond film $1\,1\,\bar{2}\,0$ lattice fringes of SiC were succeeded by 1 1 1 fringes of diamond. Polishing of the (0 0 0 1) SiC surface by ions reduced nucleation sites, and the growth rate decreased in comparison with that on the scratched surface. Fig. 2 shows an electron micrograph of a diamond film grown on a foil of the (0 0 0 1) SiC substrate polished thin enough by an ion mill to allow observation by TEM, which was free from the scratch effect of the surface. Diamonds were grown in the form of particles with hexagonal shapes. Fig. 2b is a dark field image taken by the 1 1 1 diamond reflection, indicating a single crystal diamond particle. Single crystals and polycrystals of deposited diamond particles were observed; their shapes were found to be almost identical. The orientation relationship between the SiC substrate and the diamond was determined from the electron diffraction pattern shown in Fig. 2c. Analysis of these patterns showed that a large number of orientation relationships existed. Since the lattice mismatch between diamond and SiC is not good, i.e. the misfit between them is 22%, various kinds of orientation relationships, including near-coincidence relations are possible [7]. When the deposition time was longer than that shown in Fig. 2, the particle size increased while retaining its hexagonal shape. Dislocations were not observed under and around diamond particles of SiC substrates. This suggests that the direct contact area is too small to nucleate dislocations in the SiC substrate.

WC has hexagonal close packed (HCP) crystal structure. The mismatch of lattice parameters to diamond is smaller than that of SiC. Fig. 3 shows a high resolution electron micrograph of a cross-sectional view of diamond–WC substrates. The direction of the incident electron beam was a $[1\,1\,\bar{2}\,3]$ WC substrate and the surface orientation was a $(1\,\bar{1}\,0\,1)$ plane. Again we can observe that the mixed interface structure of crystalline diamond grows directly from the WC substrate and that there is an amorphous phase between them. It can be seen from this figure that diamond was grown on the WC substrate with orientation relationships different from that of $\{h\,k\,l\} \parallel \{h\,k\,l\}$, i.e. there was no epitaxial growth of diamond on the WC substrate in the directly bonded area. Fig. 4 shows a schematic drawing of the directly bonded area in Fig. 3, in which one-dimensional fringes of (1 1 1) diamond and two-dimensional fringes of the WC substrate can be observed. At the interface, the lattice planes of the (1 1 1) diamond join atomic rows in the $[1\,1\,\bar{2}\,3]$ direction on a $(1\,\bar{1}\,0\,1)$ plane of WC with a mismatch of 23%. Every four (1 1 1) diamond planes match three planes of atomic rows in the $[1\,1\,\bar{2}\,3]$ direction of WC (we term this the 4/3 structure). When the misfit is 25%, the interface structure should be formed by the periodic 4/3 structure. It is seen from Fig. 4 that a disorder of the periodic 4/3 structure takes place and

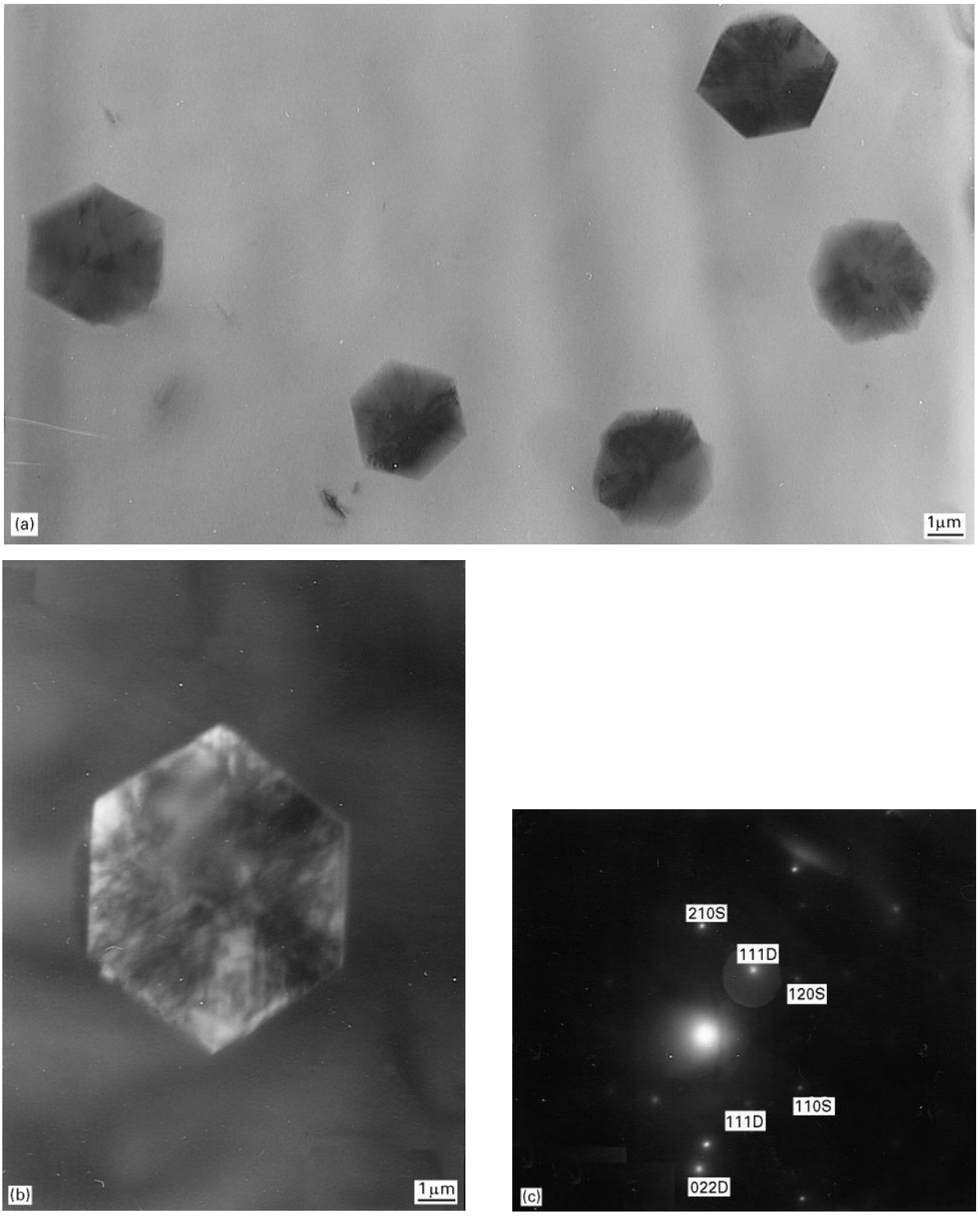

Figure 2 Electron micrograph of a diamond (D) film grown on a foil of the (0 0 0 1) SiC substrates (S) (a), dark field image taken from the 1 1 1 diamond (b), and electron diffraction pattern (c) of (a).

that the 5/4 structure is introduced into the 4/3 structure, because the misfit at the interface is smaller than 25%. Since the structure of the interface of a directly bonded area exists even when the lattice mismatch is 23% in the diamond–WC system, the diamond–SiC system, in which the misfit is nearly equal to but a little smaller than that of the diamond–WC system, may show the existence of several orientation relationships with the interface structures, such as the 4/3 structure accompanied by the 5/4 structure. Because the orientation relationship changes with a small change of the misfit, the energy cusps seem to be shallow with the change of the misfit.

When the lattice constant of a substrate becomes close to that of diamond, the growth morphology of a diamond film is quite different from that of a film grown on SiC and WC substrates. The diamond films on SiC and WC substrates at the initial stage had the form of particles as shown in Fig. 2. Fig. 5 shows an electron micrograph of the surface of a diamond film deposited on single crystal CBN, where the misfit between diamond and CBN is 1.4%. The deposited

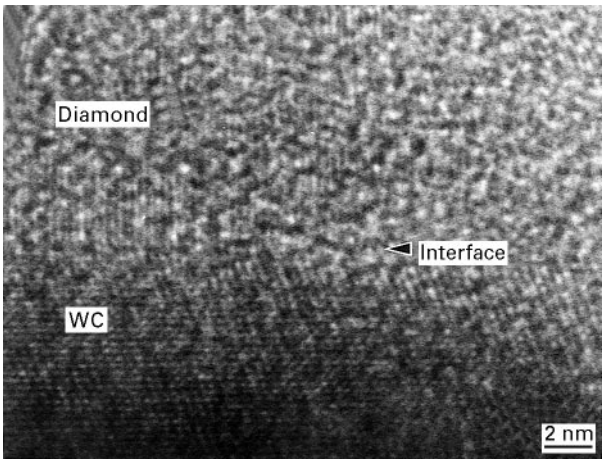

Figure 3 High resolution electron micrograph of a cross-sectional view of diamond–WC substrates.

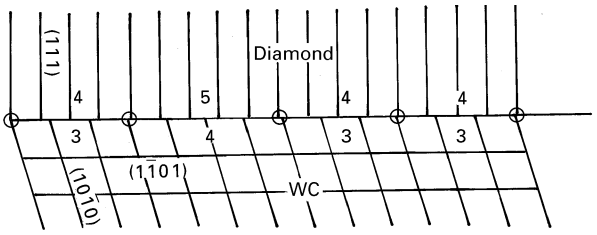

Figure 4 Schematic drawing of the directly bonded area of diamond–WC shown in Fig. 3.

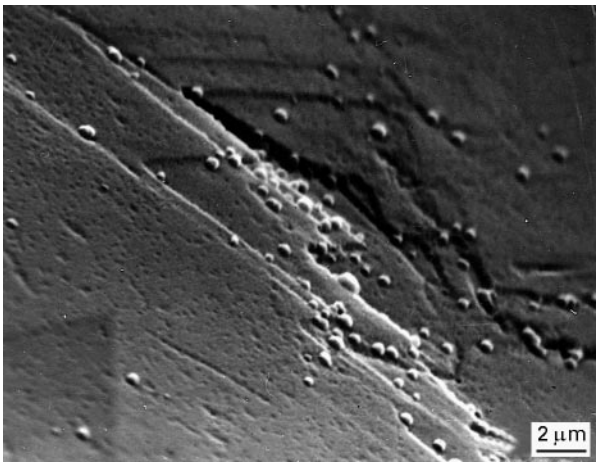

Figure 5 Electron micrograph of the surface of a diamond film deposited on a single crystal of CBN.

surface was rather flat and included growth steps, which suggested that the lateral growth of the diamond film occurred during deposition of the diamond film on CBN. Fig. 6 shows a cross-sectional electron micrograph and electron diffraction patterns of the diamond–CBN sample. The surface orientation of cubic BN was a (1 1 1) plane and the beam direction was [0 1 1]. It is clear that the dark and bright areas of the bright field image are diamond and cubic BN, respectively. The interface, divided into a dark area and a bright area, is well defined and does not seem to include an amorphous layer. The electron diffraction patterns reveal that areas have fundamentally the same pattern as the (0 1 1) incidence of the electron beam, i.e. the diamond film is grown epitaxially on CBN with the same orientation. The substrate of CBN was defect free even after deposition; on the other hand, the diamond film included defects, such as dislocations and twins, that resulted in the dark contrast with the bright field image and streaks of reflections in the diffraction pattern of the diamond film. Diamond formed a thin film rather than a particle such as that observed on SiC substrates. Since a single crystal of CBN particles was faceted and usually formed by planes of {1 0 0}, {1 1 0} and {1 1 1}, and was too small to make samples for electron microscopic observation, sintered CBN crystals were employed to observe the morphology of diamond on CBN. Fig. 7 shows an electron micrograph of an as-deposited surface of diamond on a cubic BN substrate that was scratched by a 1 μm diamond paste. After deposition, two kinds of growth morphologies were observed: one was the particle growth and the other was the layer growth. It was confirmed that particle growth occurred on the surface of the binder used for sintering cubic BN and that layer growth occurred on the surface of diamond on cubic BN. A magnified image of the surface of diamond deposited on cubic BN revealed that the diamond was rough, but retained the surface of the substrate that was scratched by the 1 μm diamond paste before deposition. As shown in Fig. 8, the surface roughness of diamond deposits caused by scratching by 1 μm diamond paste disappeared when Ar ions were used for etching prior to diamond deposition. This figure shows that the surface of diamond on the ion-milled substrate was much smoother than that deposited on scratched substrates. Fig. 9 shows electron micrographs of diamond on cubic BN scratched by 1 μm diamond paste, indicating the initial growth of diamond. In this case, cubic BN was polished and then ion-milled on only one side: the other side was deposited with diamond. The bright field image indicated that a high density of dislocations was introduced in the cubic BN substrate due to scratching by 1 μm diamond paste. Diamond was grown as particles, which showed the same growth morphology as that of diamond on the SiC substrates. Though the diamond particles seemed to be nucleated along the scratched trace, it is not clear whether the dislocations affected the nucleation of the diamond particles or not. The electron diffraction pattern and the dark field image taken by 111 revealed that bright diamond particles in the dark field image had the same orientation as the cubic BN substrate, but a few reflections different from the above relation were observed.

Fig. 10 shows the electron micrographs and electron diffraction patterns of diamond on the cubic BN substrate, which was ion milled after scratching by 1 μm diamond paste. The thin foil substrates were prepared in the same manner as shown in Fig. 9, except that the substrate was slightly ion thinned before diamond deposition. Observation was performed just after the deposition of diamond. The dark field image of the plan-view section of diamond on cubic BN revealed that the diamond deposits formed a flat and continuous film, which is different from that

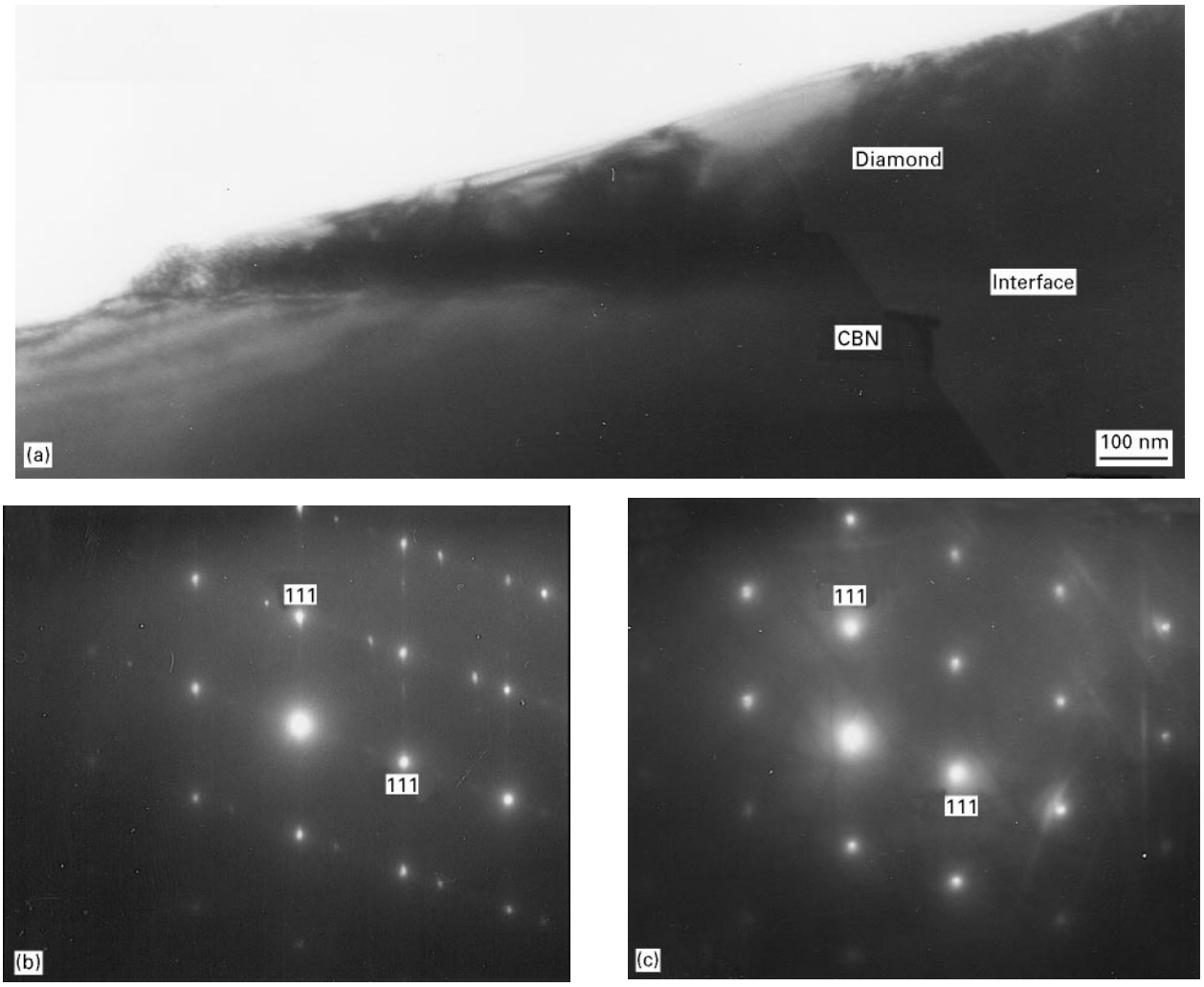

Figure 6 Cross-sectional electron micrograph (a), and electron diffraction patterns of the diamond (b) and CBN (c).

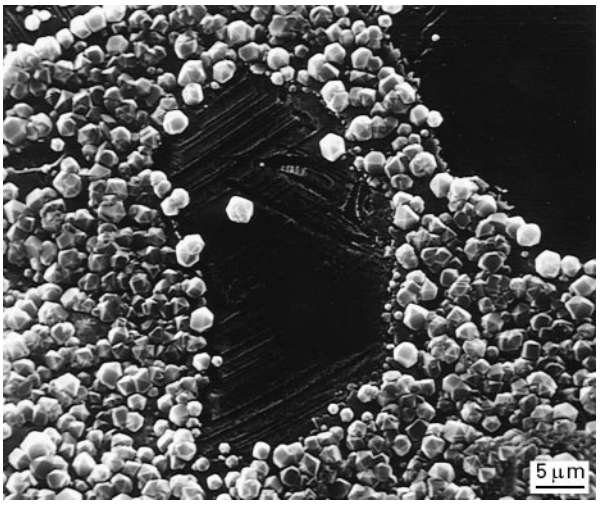

Figure 7 Electron micrograph of an as-deposited surface of diamond on the cubic BN substrate scratched by a 1 μm diamond paste.

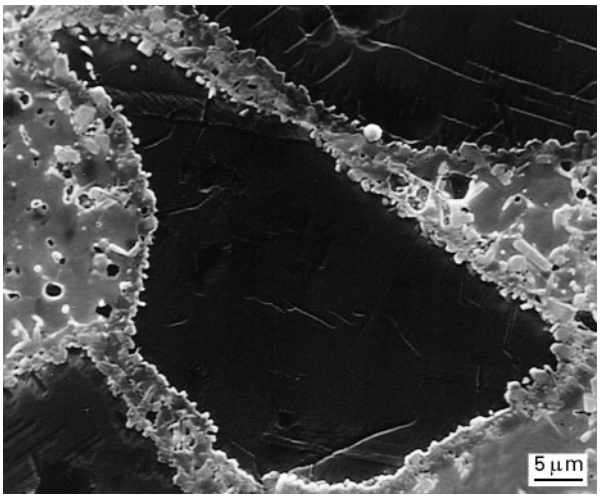

Figure 8 Surface of a diamond on the ion-milled cubic BN substrate.

of the particle growth using the scratched substrates. The electron diffraction pattern taken from a bright area in Fig. 11 shows that the incident beam direction was a 1 1 4 cubic BN, i.e. diamond was deposited on the surface of (1 1 4) cubic BN. Analysis of the electron diffraction pattern taken from the dark area in Fig. 10 indicated that the plane perpendicular to the electron beam was the (1 1 0) of diamond. This means that diamond was grown in a [1 1 0] direction on the (1 1 4) cubic BN. Since the electron diffraction pattern of the (1 1 0) diamond completely matched that of the (1 1 4) cubic BN, the orientation relationship between them

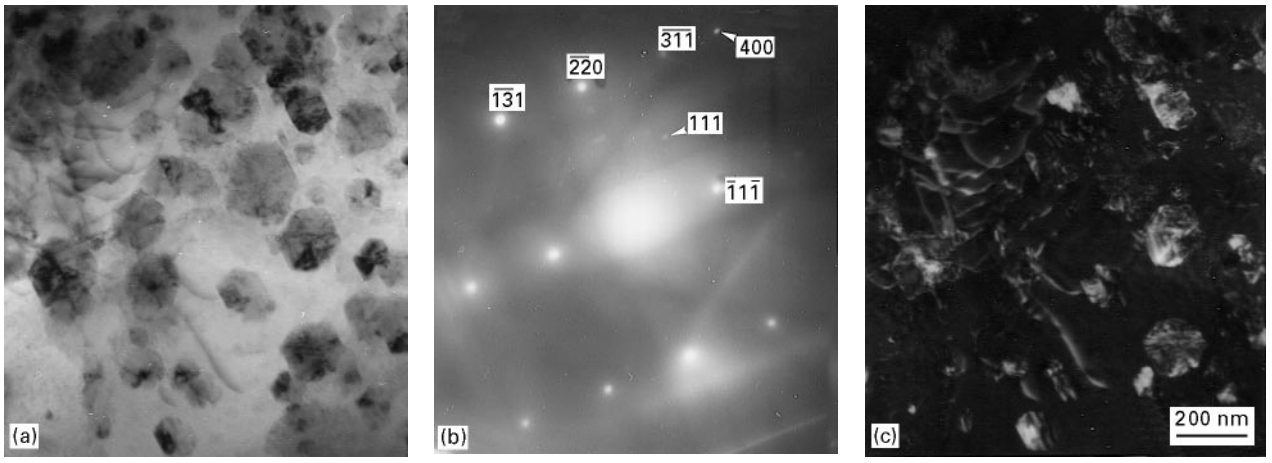

Figure 9 Electron micrograph (a), electron diffraction pattern (b), and dark field image (c) of diamond on cubic BN scratched by 1 μm diamond paste.

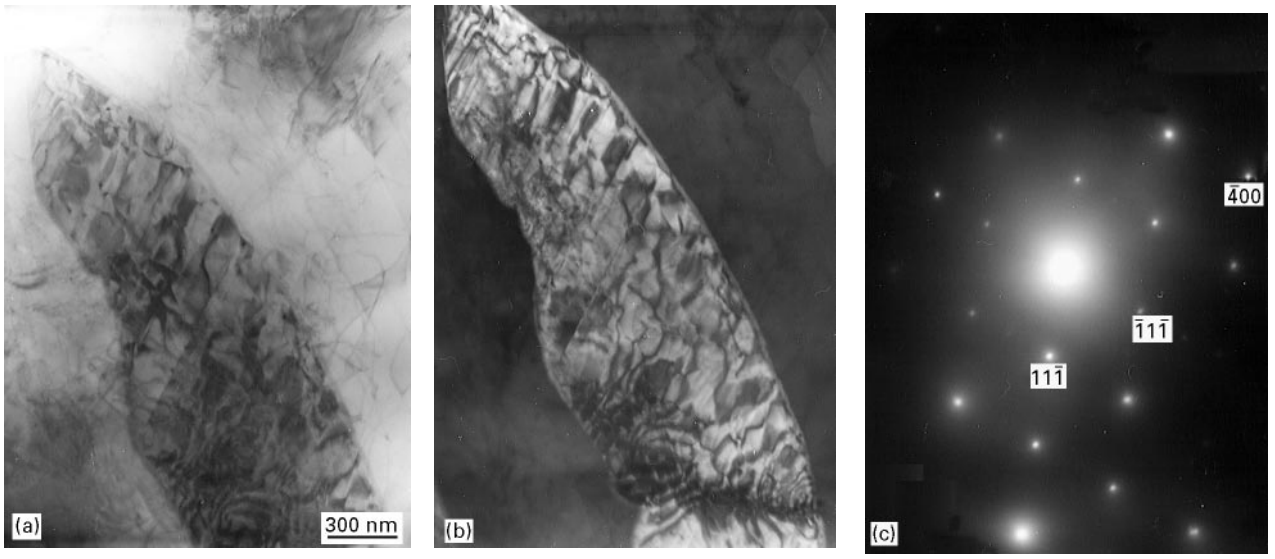

Figure 10 Bright field image (a), dark field image (b), and electron diffraction pattern (c) of diamond on the ion-polished cubic BN substrate.

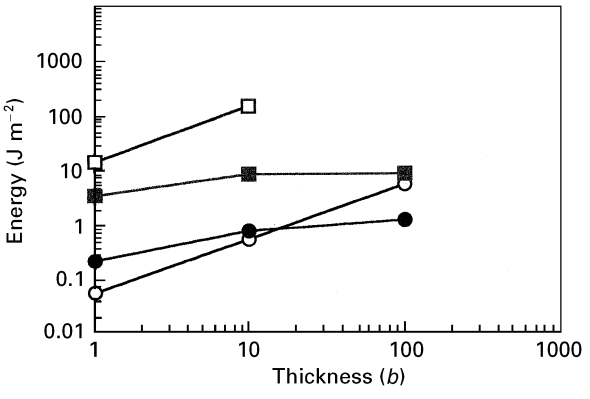

Figure 11 Thickness dependence of the elastic strain, E_e, and misfit dislocation, E_d, energies for diamond films on cubic BN and SiC substrates: For CBN: (○) E_e, (●) E_d. For SiC: (□) E_e, (■) E_d.

was (1 1 0) D||(1 1 4) CBN, [2 2 0]D||[2 2 0]CBN and [1 3 1]D||[1 3 1]CBN. The dark field image taken by the 1 1 1 reflection of diamond gave the image with bright and dark areas in the diamond film. The bright area in this figure must obey the above orientation relationship, but the dark area may be different from the above orientation relationship. Since there were no twin reflections in the diffraction pattern in Fig. 10c, this contrast was not the result of twins parallel to the beam direction.

4. Discussion

Our results can be summarized as follows:

1. when the lattice constant is large in comparison with that of diamond. i.e. the misfit is large, the interface includes an amorphous layer, though a directly bonded small area can be observed;
2. when the misfit is as small as that in the case of the diamond–cubic BN, the interface is bonded directly; and
3. ion polishing of the cubic BN surface aids the layered growth of diamond films.

This means that the nucleation of diamonds can be controlled by scratching and polishing by ions.

The growth morphology at the interface, whether it is epitaxial growth or amorphous growth, affects factors such as:

1. the formation energy of diamond and amorphous carbon;
2. the interface energy between diamond–substrates and amorphous carbon–substrates;
3. the strain energy due to epitaxial growth and
4. the misfit dislocation energy.

The third and fourth factors must be taken into account when diamond grows directly from the substrate. Matthews has discussed the strain energy of a thin film on the substrate to consider elastic misfit strain and misfit dislocations [8]. Now we consider the case where diamond grows directly from the substrate and calculate the strain energy due to the misfit. To simplify the discussion on energy, two extremely different cases are considered. The first case is a film that has completely strained itself without any introduction of misfit dislocations, and the second case is that in which the misfit strain is accommodated only by misfit dislocations. If the stress-free lattice parameters of the deposit and substrate are a_d and a_s, the misfit, f, is

$$f = (a_s - a_d)/a_d$$

The energy associated with elastic strain parallel to the film plane is

$$E_e = f^2 Bh$$

where h is the film thickness. If the film is elastically isotropic, then

$$B = 2G(1 + \nu)/(1 - \nu)$$

where G is the shear modulus and ν is Poisson's ratio.

On the other hand, when the misfit strain is accommodated by misfit dislocations, the energy of two perpendicular and non-interacting arrays of edge dislocations with separation, S, is approximately

$$E_d = Df[\ln(R/b) + 1]$$

where

$$D = G_d G_s b/\pi(G_d + G_s)(1 - \nu)$$

with b being the magnitude of the Burger's vector of the dislocation, R being the distance to the outermost boundary of the stress field of the dislocation, G_d being the shear modulus of the deposit and G_s being the shear modulus of the substrate. Fig. 11 shows the dependence of energy on thickness, indicating those for the diamond films on cubic BN and SiC substrates. In the case of CBN–diamond, the elastic strain energy is lower than that of the misfit dislocation for thicknesses of less than about $10b$. Misfit dislocations are introduced after the critical thickness of $10b$ is reached to accommodate the misfit. On the other hand, the elastic strain energy is higher than the misfit dislocation energy even when the thickness of the deposit is only one layer of diamond on the SiC substrate. However, it seems to be difficult to regard the misfit dislocation introduced into the diamond–SiC interface as the dislocation, because the distance of the dislocations is too close to overlap the dislocation cores, which are considered as a special atomic arrangement and cannot be treated by the classical elastic theory [9].

There have been few reports on the structure of amorphous carbon, though amorphous Si has been studied extensively both experimentally and theoretically. The structure of amorphous Si, which is characterized by co-ordination numbers, the deviation width of the bond angle and the cohesive energy, has been clarified [10, 11]. Though quantitative discussion is difficult because of the lack of data on amorphous carbon, it is still worthwhile considering the initial stage of the diamond growth on the SiC substrates. When diamond grows as amorphous carbon during the initial stage of film growth, the existence of the distribution of co-ordination numbers and bond angles aids the continuous growth of the amorphous film at the interface by lowering the strain energy caused by the misfit. However, as the amorphous carbon becomes thicker, the growth morphology changes from amorphous to crystalline because of the structural instability of amorphous carbon during film growth under the present experimental conditions.

References

1. G.-H. M. MA, Y. H. LEE and J. T. GLASS, *J. Mater. Res.* **5** (1990) 2367.
2. S. J. HARRIS, A. M. WEINER and T. A. PERRY, *J. Appl. Phys.* **70** (1991) 1385.
3. K. TAMAI, J. ECHIGOYA and H. SUTO, *J. Jpn Inst. Metals* **53** (1989) 1214.
4. Y. TZOU, J. BRULEY, F. ERNST, M. RUHLE and R. RAJ, *J. Mater. Res.* **9** (1994) 1566.
5. S. KOIZUMI, T. MURAKAMI, K. SUZUKI and T. INUZUKA, *Appl. Phys. Lett.* **57** (1990) 563.
6. H. SHIOMI, K. TANABE, Y. NISHIBAYASHI and N. FUJIMORI, *Jpn. J. Appl. Phys.* **29** (1990) 34.
7. W. BOLLMANN, "*Crystal Defects and Crystalline Interfaces*" (Springer-Verlag, New York, 1970) p. 143.
8. J. W. MATTHEWS, *Epitaxial Growth*, Part B. (Academic Press, New York, 1975) p. 559.
9. A. H. COTTRELL, "*Theory of Crystal Dislocations*" (Gordon & Breach, New York, 1964) p. 56.
10. S. C. MOSS and J. F. GRACZY, in Proceedings of the Tenth International Conference on the Physics of Semiconductors, edited by S. P. Keller, J. C. Hensel and F. Stern (1970) p. 658.
11. F. WOOTEN, K. WINER and D. WEAIRE, *Phys. Rev. Lett.* **54** (1985) 1392.

Received 10 October 1995
and accepted 10 February 1997